IEEE Access
Multidisciplinary | Rapid Review | Open Access Journal

Received 14 May 2023, accepted 19 May 2023, date of publication 24 May 2023, date of current version 1 June 2023.

Digital Object Identifier 10.1109/ACCESS.2023.3279307

RESEARCH ARTICLE

Statistically Inspired Passivity Preserving Model Order Reduction

NAMRA AKRAM[1], MEHBOOB ALAM[2], (Member, IEEE), RASHIDA HUSSAIN[1], AND YEHIA MASSOUD[3], (Fellow, IEEE)

[1]Department of Mathematics, Mirpur University of Science and Technology (MUST), Mirpur, Azad Jammu and Kashmir 10250, Pakistan
[2]Department of Electrical Engineering, University of Poonch Rawalakot, Rawalakot, Azad Jammu and Kashmir 12350, Pakistan
[3]Innovative Technologies Laboratories (ITL), King Abdullah University of Science and Technology (KAUST), Thuwal 23955, Saudi Arabia

Corresponding author: Yehia Massoud (yehia.massoud@kaust.edu.sa)

This work was supported in part by the Mirpur University of Science and Technology (MUST), Mirpur, Azad Jammu and Kashmir, Pakistan; in part by the University of Poonch Rawalakot, Azad Jammu and Kashmir; and in part by the King Abdullah University of Science and Technology (KAUST), Thuwal, Saudi Arabia.

ABSTRACT The continuous scaling of the on-chip devices and interconnects increases the complexity of the design space and becomes a crucial factor in the fabrication of modern integrated circuits. The ever decreasing of interconnect pitch along with process enhancement into the nanometer regime had shifted the paradigm from a device-dominated to an interconnect-dominated methodology. In the design methodology, Model Order Reduction (MOR) reduces the size of large-scale simulation of on-chip interconnect to speed up the performance of design tools and chip validation. In approximating the original system, the passivity preserving MOR technique of using spectral zeros as positive real interpolation points preserves the stability and passivity of the system. In this work, statistical distribution techniques are proposed for the selection of spectral zeros. The proposed method is based on using the gaussian, uniform, binomial, and weibull distributions to select spectral zeros to better match moments with the least absolute error between the original and reduced-order systems. The results show that the reduced-order model developed using the Gaussian distributed Spectral zeros Projection (GSP) method offers higher accuracy and numerical stability compared to other distributions.

INDEX TERMS Statistical distribution, model order reduction, passivity preserving, spectral zeros, on-chip interconnects, computer aided design.

I. INTRODUCTION

Over the last several decades, the complexity and requirement of physical layout and verification flow presented great challenges for the development and fabrication of modern integrated circuits [1]. The on-chip devices scaling and interconnects resulted in an exponential rise in design complexity with increased simulation time [2], [3]. While creating large-scale systems, the physical behavior can often be simplified and represented by a system of mathematical equations [4], [5], [6], [7]. Modeling of the on-chip devices and interconnect often resulted in a large-scale system of differential equations, thereby making it essential to replace it with a lower-order approximation for testing and design verification. The modern design tools for the simulation of on-chip interconnect are numerically expensive and often lack passivity preserving approximation of on-chip systems [8], [9]. In recent decades, complex and large-scale Model Order Reduction (MOR) has been a subject of major interest [10], [11], [12], [13], [14]. These large-scale systems extract sparse matrices and have a positive real transfer function, which necessitates the use of MOR approaches that preserve passivity for the approximate solution of the original system. In addition, the reduction technique needs to meet the strict requirements for accuracy, stability, and low complexity.

The two main classifications of the MOR techniques for on-chip interconnect are projection and non-projection-based methods [15], [16], [17]. The most prominent include Krylov subspace and singular value decomposition (SVD) based projection methods, whereas Hankle-norm approximation

The associate editor coordinating the review of this manuscript and approving it for publication was Wen-Sheng Zhao.

is the popular non-projection method [18]. In application-specific solutions, the design often necessitates strict system theoretic requirements to be fulfilled by the reduced order model (ROM). The accuracy of the original system and the number of reduced state variables properly adhering to the terminal behavior are two necessary factors for the reduced model [11], [19]. Recently, the preservation of passivity of the original system in MOR for on-chip interconnect systems is a topic of great interest and importance for design verification and validation [20], [21]. It is important to observe here that on-chip interconnects are inherently passive, however, the non-passive Reduced Order Model (ROM) can produce unwanted behavior at operating frequencies, resulting in an unstable system. Note that passivity implies stability, but vice versa is not true.

The interconnect systems we consider in this study are passive and stable, and it is preferred that the theoretical features of passivity and stability of the original system must be kept in the reduced model. Keep in mind that combining a stable but non-passive original system with passive components frequently results in the system becoming unstable [22], [23]. There are primarily two categories of passivity-preserving MOR for on-chip interconnect systems. The first method uses SVD-based balance reduction, and the second way uses Krylov subspace methods to develop reduce order models [24], [25], [26]. As compared to SVD-based reduction techniques, the Krylov subspace approaches are effective and demonstrate a better estimate of the ROM [27]. The Passive Reduced-Order Interconnect Macromodeling Algorithm (PRIMA) and its variant Structure-Preserving Reduced-Order Interconnect Macromodell (SPRIM) are two main methods using congruence transformations for generating a reduced model via Krylov sub-space projection [25], [28]. In general, the Krylov methods use reachability subspaces for generating vector sequences to subsequently build projection matrices. Essentially, these are the iteration-based method, which in some sense approximate the eigenvalues of the original system to match moments to generate a reduced system.

In the MOR techniques, different types of algorithms exist based on Krylov-subspace methods [29], [30], [31]. They are computationally inexpensive and desirable because of their iterative nature as opposed to balanced approximations [32], [33]. Nevertheless, Krylov-based approximation techniques only take into account one moment of every iteration and can lead to lower accuracy at a certain point [12]. In addition, contrary to the balanced approximation, stability is not always guaranteed, and there are no error boundaries in the system approximation. The balanced approximations methods, such as FABT [34], [35], PMTBR [36], [37] and PRTBR [38] are SVD-based approaches in passivity-preserving MOR. These methods demand intensive computations such as n^2 and n^3 and are not appropriate for reducing large-scale systems [39]. An SVD-based projection method using spectral zero (SZ) is recently introduced, where in order to generate the simplified model, the interpolation points are chosen using spectral zeros [40], [41]. Selecting the spectral zeros for a match is still a research problem under consideration. A selection criterion supported by dominant spectral zeros was initially proposed, based on the residuals connected with the dominant poles of the system [42]. However, spectral zero selection using the dominant pole is computationally intensive. We may alternately select spectral zero via the frequency selective reduce norm spectral zero (RNSZ) method [43]. In the RNSZ method, the frequency intervals are uniformly placed over the frequency of interest, and the SZs are chosen on the basis of their dominance in the reduced norm sense. However, in this work, we argue that many natural phenomena either follow or can be approximated to follow a statistical distribution. Note that the distribution is used to select spectral zero to get a better match of the moments with the least absolute error between the original and reduced-order system. It is useful to note that the RNSZ projection via-spectral zeros is frequency selective projection and only reasonably accurate across a certain, limited frequency range. The primary contributions of this paper are

- Formulation of a new MOR projection method, where spectral zeros are selected via various statistical distribution techniques. Among these techniques, Gaussian distributed Spectral zeros Projection (GSP) is finally preferred, which is numerically efficient and offers higher accuracy and numerical stability compared to other distribution methods.
- All statistical distribution techniques are simulated using several examples of on-chip interconnects. The results of the GSP method show improved moment matching with reduced absolute error for the reduce-order model generated by other distribution methods.

The problem formulation of passivity preserving model order reduction techniques is discussed in the next section. The derivation with the pseudocode of the proposed method for reducing the model using a Gaussian distributed spectral zero projection is explained in Section III. Simulations and analysis are discussed in Section IV. Section V finally concludes the paper.

II. PASSIVITY PRESERVING MODEL ORDER REDUCTION FOR ON-CHIP INTERCONNECTS

Recent advances in integrated circuit manufacturing are ultimately transforming the computer-aided design (CAD) industry [44]. MOR reduces the original system and speeds up the numerical simulation of complex design in a CAD tool [45]. In the general state-space form of the MOR of on-chip interconnect the developed set of equations is a function of independent time and space variables. The state matrices account for the complex electromagnetic 3D effects, which are derived using Maxwell's equations and extracted by field solvers [46], [47], [48]. Note that the state matrices, sparsely populated with resistors, inductors, and capacitors are analogous to transmission line lumped components, which accounts for their distributed effects.

In the design of integrated circuits, understanding the system helps in converting these effects into a set of ordinary differential equations. The set of equations can be rearranged to construct state space formulation of the linear dynamical system as [40]

$$\begin{aligned} C_{cell}\dot{x} &= G_{cell}x(t) + B_{cell}u(t), \\ y(t) &= L_{cell}x(t) + D_{cell}u(t), \end{aligned} \tag{1}$$

where $x(t) \in \mathbb{R}^n$ shows the state variables, $u(t) \in \mathbb{R}^m$, and $y(t) \in \mathbb{R}^p$ represents the input and output of the system respectively. Similarly, C_{cell}, $G_{cell} \in \mathbb{R}^{n\times n}$, ($G_{cell}$, C_{cell}) shows the generalized eigenvalues of the system, $B_{cell} \in \mathbb{R}^{n\times m}$, $L_{cell} \in \mathbb{R}^{p\times n}$, $D_{cell} \in \mathbb{R}^{p\times m}$ are the linear mapping matrices between inputs, output and state variables. It is important to observe that the state-space model shown in Eq.(1) accounts for all on-chip interconnect capacitance, inductance, and resistance effects. Resistance (R), inductance (L), and capacitance (C) block arrays are represented in the state space form as

$$\begin{aligned} \underbrace{\left[\begin{array}{c|c} C & 0 \\ \hline 0 & L \end{array}\right]}_{C_{cell}} \dot{x}(t) &= \underbrace{\left[\begin{array}{c|c} R & \\ \hline & 0 \end{array}\right]}_{G_{cell}} x(t) + \underbrace{\left[\begin{array}{c} \\ \hline \\ \hline \end{array}\right]}_{B_{cell}} u(t), \\ y(t) &= \underbrace{\left[\begin{array}{c} \\ \hline \\ \hline \end{array}\right]}_{B_{cell}^T = L_{cell}} x(t) + \underbrace{\left[\begin{array}{c} \\ \hline \\ \hline \end{array}\right]}_{D_{cell}} u(t). \end{aligned} \tag{2}$$

The aim of approximating the original system is to readopt the system's dynamics to a lower-order dimensional subspace i.e. $k \ll n$, where n and k are the order of the original and reduced order system respectively. The model of order k corresponding to Eq. (1) is given as

$$\begin{aligned} \hat{C}_{cell}\dot{\hat{x}} &= \hat{G}_{cell}\hat{x}(t) + \hat{B}_{cell}u(t), \\ \hat{y}(t) &= \hat{L}_{cell}\hat{x}(t) + D_{cell}u(t), \end{aligned} \tag{3}$$

where $\hat{x} \in \mathbb{R}^k$, $\hat{C}_{cell} \in \mathbb{R}^{k\times k}$, $\hat{G}_{cell} \in \mathbb{R}^{k\times k}$, $\hat{B}_{cell} \in \mathbb{R}^{k\times m}$, $\hat{L}_{cell} \in \mathbb{R}^{p\times k}$, $D_{cell} \in \mathbb{R}^{p\times m}$. It is likewise clear that the system theoretical properties of the original system i.e. stability and passivity should be preserved by the ROM. Given that passive systems don't produce power, the stability and preservation of passivity of the ROM is important in MOR. The property of positive real transfer function can guarantee passivity in ROM and is used in the proposed method [11]. The projection matrices U and V are often used in MOR to generate the ROM such that $U, V \in \mathbb{R}^{n\times k}$, and $V^T U = I_k$. Proper selection of U and V not only preserves the system's properties (passivity, stability) but also ensures that ROM keeps the dynamics of the system. The matrices U and V operate on original system state matrices to construct the ROM and can be represented as:

$$\begin{aligned} \hat{C}_{cell} &= V^T C_{cell} U, \quad \hat{G}_{cell} = V^T G_{cell} U, \\ \hat{B}_{cell} &= V^T B_{cell}, \quad \hat{L}_{cell} = L_{cell} U. \end{aligned} \tag{4}$$

The invertible and non-invertible C_{cell} matrices are contained in the initial system definition of the state representation of on-chip interconnects. It should be noted that due to some of the system poles and spectral zeros being at infinity, a singular C_{cell} matrix poses a unique set of difficulties. Therefore, the invertible and non-invertible matrices in MOR are treated separately [49], [50]. In the state definition, C_{cell} is an invertible non-singular matrix as extracted by full-wave field solvers for on-chip interconnect [46], [47], [48].

Definition of Passivity: The system's A linear time-invariant (LTI) system is said to be passive if the following conditions of transfer function $P(s)$ are true [11]

- $P(s)$ is analytic for $\mathbb{R}e(s) > 0$;
- $P(\bar{s}) = \overline{P(s)}\ \forall\ s \in \mathbb{C}$;
- $P(s) + P(-s)^T \geq 0$ for $\mathbb{R}e(s) > 0$.

Hence, we always have for real system $P(\bar{s}) = \overline{P(s)}$ and the third property shows the presence of the stable matrix function $W(s)$, which satisfies the condition $P(s) + P^T(-s) = W(s)\ W^T(-s)$ and the spectral factorization of P, and W are the spectral factors of P. The spectral zeros of P are derived from the zeros of W, i.e., Λ_i, for $i = 1, \cdots, n$, : $\det W(\Lambda_i) = 0$.

III. PASSIVITY PRESERVING MOR USING STATISTICAL DISTRIBUTION

In this section, we explain the derivation and procedure of the proposed use of statistical distribution for passivity-preserving MOR. Note that among the proposed distribution, the gaussianly distributed spectral zeros projection method outperforms other distribution methods in accuracy and absolute error of the ROM. Our proposed passivity-preserving MOR method is based on LTI systems with a frequency-selective positive real interpolation that uses stable spectral zeros, to construct the projection matrices. The technique is inspired by natural phenomena, which either follow or can be approximated to follow a statistical distribution. Note that the distribution is used to select spectral zero to get a better match of the moments with the least absolute error between the original and ROM system. The selection of spectral zeros using Gaussian distribution ensures passivity preservation and can generate a lower-order model in comparison to other distribution methods.

The derivation of the passivity-preserving MOR using various statistical distributions follows the same procedure. Therefore, without loss of generality, it is convenient to only give the derivation and subsequent explanation of the pseudocode of the Gaussian distributed spectral zeros projection method, which outperforms others i.e. binomial, weibull, and uniform distributions. Additionally, in this section, the main focus is to see how the ROM generated by the gaussianly distributed selected spectral zeros performs and guarantees the essential properties of the original system. It is often required to first review some basic system parameters and their properties that go into the derivation of the proposed method. The Laplace transform of a given transfer function $\sum$ for a system Eq.(1) can be written as

$$P(s) = L_{cell}(sC_{cell} - G_{cell})^{-1}B_{cell} + D_{cell}. \tag{5}$$

It is noted that the system poles can be found from the generalized eigen-values of the pair (G_{cell}, C_{cell}). The matrix

$(G_{cell} - \Lambda C_{cell})$ is considered non-singular for $\Lambda \in \mathbb{C}$ [51], and is reflected as matrix pencil $(G_{cell},\ C_{cell})$. All of the system's finite poles must be located inside the left half of the s-plane in order for the system $\sum$ to be considered stable, that is $\mathrm{Re}(\Lambda) < 0$ with $|\Lambda| \neq \infty$. Note that the spectral zeros of $\sum$ are all $s \in \mathbb{C}$, i.e. $\det [P(s) + P^T(-s)] = 0$, whereas

$$P^T(-s) = B_{cell}^T(-sC_{cell}^T - G_{cell}^T)^{-1}L_{cell}^T + D_{cell}^T. \quad (6)$$

The SZ has a reflection in the s-plane, as demonstrated by this definition. Note that the real SZs s_i exists in pairs $(s_i, -s_i)$, whereas the complex ones exist in quadruples $(s_i, s_i^T, -s_i, -s_i^T)$. In addition, these definitions demonstrate that the transfer function is positively real, and as a result, when The system preserves the ROM's passivity by creating projection matrices using spectral zeros. It is important here to formally define Spectral Zeros (SZs). They are zeros of the follwing square system (7), which are the eigenvalues of the matrix $[G_{cell} - B_{cell}D_{cell}^{-1}L_{cell}]$.

$$\left[\begin{array}{c|c} G_{cell} & B_{cell} \\ \hline L_{cell} & D_{cell} \end{array}\right] \quad (7)$$

This is essentially the motivation for our proposed GSP method to preserve frequency-selective passivity. The method divides the frequency limits into regular intervals and selects the stable spectral zeros, which are guassianly distributed in the area of interest. Note that the interested area is usually application specific, and accounts for the range of frequency, where we want the response of the ROM with reasonable accuracy. The stable SZs of the system are derived from the partial fraction expansion $P(s) + P(-s)^T$ of $P(s)$. The selected spectral zeros become the interpolation point to build projection matrices (U and V) that equally ensure the passivity and stability of the system and also generate the application specific ROM. Firstly, the GSP method finds the $\bar{\mathrm{H}}$ and $\bar{\mathrm{E}}$ matrix form the original state representation Eq.(1), and can be expressed as

$$\bar{\mathrm{H}} := \begin{bmatrix} G_{cell} & & B_{cell} \\ & & -G_{cell}^T & -L_{cell}^T \\ L_{cell} & B_{cell}^T & D_{cell} + D_{cell}^T & \end{bmatrix}, \quad (8)$$

$$\text{and} \quad \bar{\mathrm{E}} := \begin{bmatrix} I & & \\ & I & \\ & & 0 \end{bmatrix}. \quad (9)$$

The matrices $\bar{\mathrm{H}}$ and $\bar{\mathrm{E}}$ are used to extract the generalized eigenvalue problem that is the finite eigenvalues. Note that the finite spectral zeros as a subset of eigenvalues are complex numbers Λ of the matrix $\bar{\mathrm{H}}$, i.e. Rank $(\bar{\mathrm{H}} - \Lambda\bar{\mathrm{E}}) < 2n + p$, which is similar to finding a solution to the finite generalized eigenvalues $\Lambda(\bar{\mathrm{H}}, \bar{\mathrm{E}})$. Therefore, the pair gives projection vectors U and V, which are basically generated using statistical distribution and also maintain the passivity of the ROM.

A. PSEUDOCODE FOR GAUSSIAN DISTRIBUTED SPECTRAL ZEROS PROJECTION

In the previous section, the passivity-preserving projection was explained and defined the essential task of building the matrices U and V. The U and V are compiled by the chosen SZs, which are part of original system's n stable SZs. Note that the proposed technique (GSP) of selecting the spectral zeros uses the Gaussian distribution associated with the mean value of the SZs. The selected SZs are used to construct matrices U and V and determines the accuracy of the ROM. This section explains the pseudo-code of the GSP method, with all the essential guides to execute in any language. The pseudo-code of the GSP is explained in **Algorithm** 1 . The inputs for the principal function are the state matrices of the original system, i.e. C_{cell}, G_{cell}, B_{cell}, L_{cell}, and D_{cell}. In the first step of the algorithm, factorization [Q, R] is performed to calculate the systems eigenvalues and eigenvector. The SZs of the system are the generalized eigenvalues of the following formulation

$$(\bar{\mathrm{H}} - R\bar{\mathrm{E}})Q = 0, \quad (10)$$

where $\bar{\mathrm{H}}$ and $\bar{\mathrm{E}}$ are explained by Eq.(8) and (9). The Q and R are the eigenvectors and eigenvalues matrices, while the spectral zeros are the diagonal elements of R. The proposed GSP method is a frequency-selective projection of a dynamic system. The SZs of $\sum$ are the poles of $P(s)$ and the proposed criteria for selecting the SZs is their statistical dominance.

In the proposed method, Gaussian-distributed spectral zeros are selected in the minimum and maximum range of the frequency interval. The spectral zeros are selected using the *Nth* interval of frequency and is given by

$$N_p = n_{min} + 2(n_{max} - n_{min}) \sum \left(\frac{k : T}{T}\right), \quad (11)$$

where k represents the order of the ROM, T defines the value of the selected Gaussian distribution frequency point, and n_{max} and n_{min} show the minimum and maximum of the selected frequency range. Note that in the classical sense, normal distribution does not have limits. However, we can limit it by using the central limit theorem and can write generated frequency points as in (13). In using (13), the entire frequency range of interest is divided into gaussianly distributed interpolation points. Note that in normal distribution equally selected points exist above and below the means of a data set. In addition, more interpolation points exist near the mean with more than 95% falling within two standard deviations. Essentially, the selected spectral zeros out of all are based on the following criteria

$$\mathrm{SZ}_{GSP} \ = \ N_p - |img(SZ)|. \quad (12)$$

The corresponding eigenvectors based on the stable spectral zeros in developing the reduced-order model i.e. $[\bar{Q}_{xk}, \bar{S}, \bar{Q}_{yk}] = \mathrm{svd}(\mathrm{X}^T\mathrm{Y})$. The system's projection vectors U and V are then created using the eigenvectors of the chosen spectral zeros as

$$U = X\bar{Q}_{xk}\bar{S}^{-1}, \quad V = Y\bar{Q}_{yk}\bar{S}^{-1}. \quad (13)$$

It is interesting to note that these projection matrices satisfy the orthogonality requirement in addition to dynamically generating ROM. This is a generalization of our suggested

GSP method's projection approximation. To illustrate further the implementation details of the GSP method, consider the following example of order $n = 5$ with a simple rational function $\mathbf{P}(s)$.

Example 1: In this example, we take a linear time dynamical system of order $n = 5$, with its transfer function $\mathbf{P}(s)$ expressed as

$$P(s) = \frac{5s^4 + 40s^3 + 26s^2 + 8s + 1}{(s+1)^5}. \tag{14}$$

The system in state form is expressed as [11],

$$G_{cell} = \begin{bmatrix} 0 & 1 & 0 & 0 & 0 \\ 0 & 0 & 1 & 0 & 0 \\ 0 & 0 & 0 & 1 & 0 \\ 0 & 0 & 0 & 0 & 1 \\ -1 & -5 & -10 & -10 & -5 \end{bmatrix}, B_{cell} = \begin{bmatrix} 0 \\ 0 \\ 0 \\ 0 \\ 1 \end{bmatrix},$$

$$L_{cell} = \begin{bmatrix} 1 & 8 & 26 & 40 & 5 \end{bmatrix}, C_{cell} = \begin{bmatrix} 1 & 0 & 0 & 0 & 0 \\ 0 & 1 & 0 & 0 & 0 \\ 0 & 0 & 1 & 0 & 0 \\ 0 & 0 & 0 & 1 & 0 \\ 0 & 0 & 0 & 0 & 1 \end{bmatrix},$$

$$D_{cell} = 0.$$

The zeros of the $P(s) + P(-s)$ are the SZs of the original system. The calculated spectral zeros are given as
$SZ = 10^{+8}$ [0.3445 + 0.0000i, 0.2364 + 0.3696i, 0.2364 − 0.3696i, -0.0000 + 3.8932i, -0.0000 − 3.8932i, -0.2364 + 0.3696i, -0.2364 − 0.3696i, -0.3445 + 0.0000i].
Using GSP method of selecting spectral zeros as explained in Algorithm 1, the selected SZs within the range n_{min} = 1x10^8 and n_{max}=4x10^{10} are
$SZ = 10^{+8}$ [-0.0000 + 3.8932i, -0.0000 − 3.8932i, -0.2364 + 0.3696i].
It is worth noting that the corresponding eigenvectors based on the selected SZs construct the projection matrices U and V using Eq.(13). Essentially, our problem now is to use these projection matrices U, V to generate the ROM of the system using Eq.(4). The reduced ROM of order $n = 3$ is given as

$$\hat{G}_{cell} = \begin{bmatrix} 0 & -0.0000 & 0.0000 \\ 0.0000 & 1.0122 & -0.4472 \\ -0.0000 & -0.1529 & 0.5472 \end{bmatrix},$$

$$\hat{B}_{cell} = \begin{bmatrix} -2.4152 \\ 0.0000 \\ -0.0000 \end{bmatrix},$$

$$\hat{L}_{cell} = \begin{bmatrix} 2.4152 & 0.0000 & 0 \end{bmatrix},$$

$$\hat{C}_{cell} = \begin{bmatrix} 1.0000 & -0.0000 & 0.0000 \\ 0.0000 & 1.0000 & 0.0000 \\ -0.0000 & 0.0000 & 1.0000 \end{bmatrix}, \hat{D}_{cell} = 0.$$

It is important to observe here that GSP methods can be used for the approximation of systems in other engineering applications. In the Appendix at the end, we briefly discuss the interconversion of state-space and rational function representation of frequency-domain systems. Note that the GSP technique is more appropriate for fitting functions, where the interpolation points are chosen as bases of approximation. The system, with representation in either state-space or rational function, can take benefit of the proposed method.

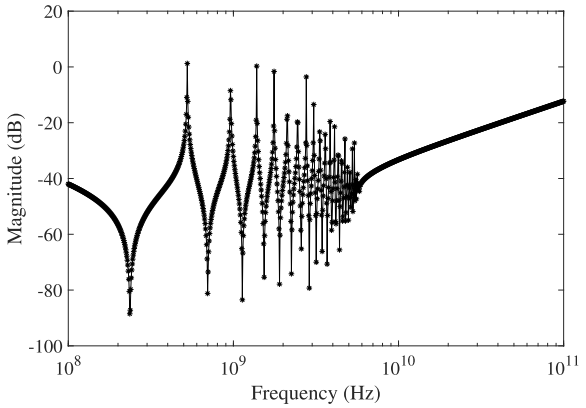

FIGURE 1. The response of a small conductor with order n=79.

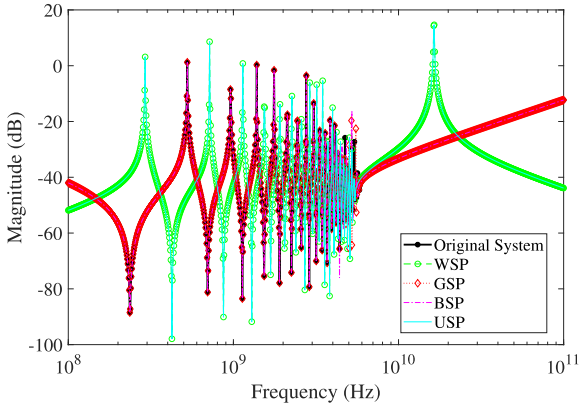

FIGURE 2. The response of a small conductor with original system order of n=79. The reduced models using GSP, BSP, WSP, and USP are of order k = 40. The result of the GSP method shows a close match with the original system in comparison to other distributions.

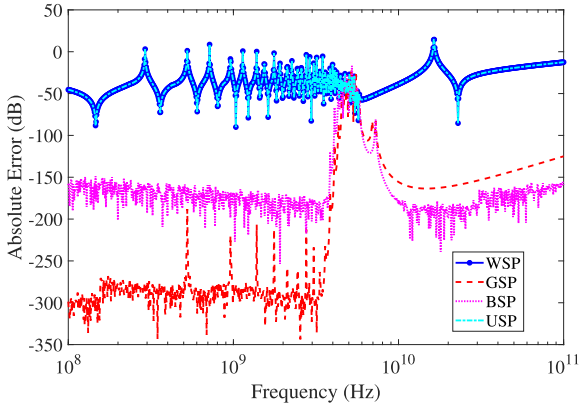

FIGURE 3. The absolute error of the reduced orders compared to the original system for the small conductor example using various statistical methods for the selection of spectral zeros. The calculated mean absolute error is -35.13 dB, −213.06 dB, −165.19 dB, and −35.13 dB for WSP, GSP, BSP, and USP methods respectively.

IV. SIMULATION AND RESULTS

In this section, the accuracy, and performance of the proposed GSP (Gaussianly distributed Spectral zeros Projection) method are compared with other statistical distribution

Algorithm 1 Pseudocode of Gaussianly Distributed Spectral Zeros

INPUT = $(C_{cell}, G_{cell}, B_{cell}, L_{cell}, D_{cell}, k, n_{min}, n_{max})$
OUTPUT = $(\hat{C}_{cell}, \hat{G}_{cell}, \hat{B}_{cell}, \hat{L}_{cell}, \hat{D}_{cell})$
Function $[\hat{C}_{cell}, \hat{G}_{cell}, \hat{B}_{cell}, \hat{L}_{cell}, \hat{D}_{cell}\ ]$ = GSP $(C_{cell}, G_{cell}, B_{cell}, L_{cell}, D_{cell}, n_{min}, n_{max}, k)$
Construct $\bar{H}$ and $\bar{E}$ from (C_{cell},G_{cell}, B_{cell}, L_{cell}, D_{cell})
Perform QR decomposition of R : [Q, R] = qr ($\bar{H}$, $\bar{E}$)
Spectral Zeros of the system SZ = diag (R)
Define n_{min}, n_{max} : Range of min and max frequency
k: Reduced Order of the system
T: Gaussian distribution frequency point
Divide limits of frequency into Nth interval of frequency: $N_p = n_{min} + 2(n_{max} - n_{min}) \sum \left(\frac{k:T}{T}\right)$,
Select Spectral Zeros
for $p = 1: k$
$SZ_{GSP} = N_P$-$|img(SZ)|$
end
Generate $\bar{S}$ and $\bar{Q}$ using selected spectral zeros and their corresponding eigenvectors,
$[\bar{Q}_{xk}, \bar{S}, \bar{Q}_{yk}] = \text{svd}(X^T Y)$
Construct Projection Matrices U and V
$U = X \bar{Q}_{xk}\ \bar{S}^{-1}, \quad V = Y\ \bar{Q}_{yk}\ \bar{S}^{-1}$
Generate Reduce order Model
$\hat{C}_{cell} = V^T C_{cell} U; \hat{G}_{cell} = V^T G_{cell} U; \hat{B}_{cell} = V^T B_{cell}; \hat{L}_{cell} = L_{cell} U; \hat{D}_{cell} = D_{cell}$

techniques. The numerical simulation analysis is carried out using Matlab and three design examples of on-chip interconnect structures are selected to include a small conductor, spiral inductor, and RLC network. These interconnect examples are built using field solvers FastCap [46] and FastHenry [47], which are capacitance and inductance extraction tools respectively. These fast field solvers use the modified nodal analysis to construct representation as shown in Eq.(1). The order of the generated examples of small conductor, spiral inductor, and RLC network are 79, 191, and 1202 respectively.

The first example is of a small conductor with an original order of 79. Note that the state matrices defined in Eq.1, are populated with extracted passive components using field solvers as shown in Eq.2. In this example, the ROM is generated using spectral zeros selected by applying gaussian, binomial, weibull, and uniform distributions. In the comparison, we define the result of the selection of spectral zero using various statistical distributions as follows

- GSP: Gaussianly distributed Spectral zeros Projection.
- BSP: Binomialy distributed Spectral zeros Projection.
- WSP: Weibully distributed Spectral zeros Projection.
- USP: Uniformly distributed Spectral zeros Projection.

It is important to define here some of the error indexes used in simulation and analysis.

- Absolute Error: It is the absolute difference between the value of the reduced and original model computed at various wavelengths.
- Mean Absolute Error: It is the mean of the absolute error computed at various wavelengths.

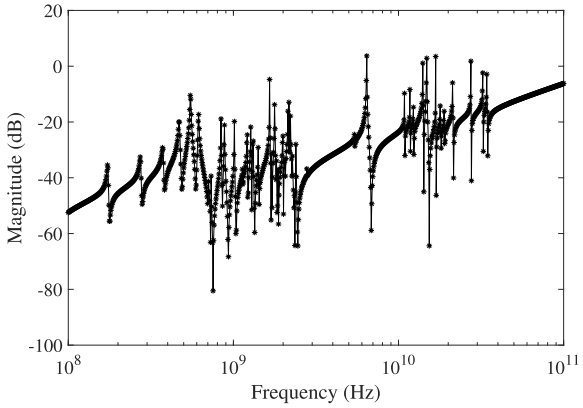

FIGURE 4. The system response generated by the spiral inductor with order $n = 191$.

- Absolute Maximum and Minimum Error: It is the maximum and minimum of the absolute error computed at various wavelengths.

The original system frequency response of the small conductor of order $n = 79$ is shown in FIGURE 1. The comparison of the projected reduced model of order $k = 40$ using the proposed GSP method with other statistical distributions is given in FIGURE 2, which is showing a better response compared to other distributions. The absolute error comparison of all distributions is given in FIGURE 3, which also shows a good match of the GSP method with the original system.

The better performance of the GSP method is further highlighted by its detailed comparison with other statistical distributions given in TABLE 1. The results in the table show that the GSP method has a Minimum Mean error of -213.06dB. In addition, it also shows reduced Minimum and

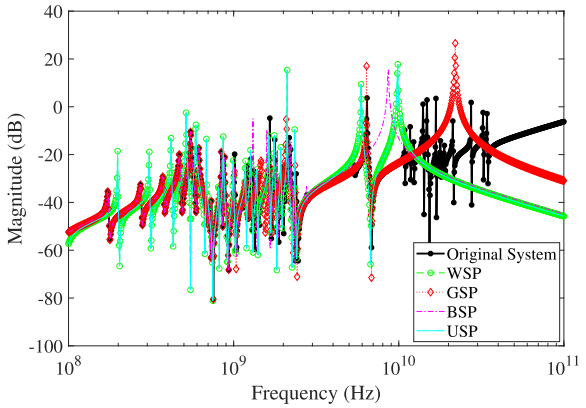

FIGURE 5. The response of a spiral inductor with the original system of order $n = 191$. The reduced models using GSP, BSP, WSP, and USP methods are of order $k = 40$. The ROM generated by the GSP method shows a close match with the original system in comparison to other distributions.

TABLE 1. Error Comparison of Small Conductor Example.

Distributions	Minimum Error	Mean Error	Maximum Error
WSP	− 90.08 dB	− 35.13 dB	14.61 dB
GSP	−337.15 dB	− 213.06 dB	− 20.17 dB
BSP	−242.04 dB	− 165.19 dB	− 17.48 dB
USP	− 90.08 dB	−35.13 dB	14.61 dB

TABLE 2. Error Comparison of Spiral Inductor Example.

Distributions	Minimum Error	Mean Error	Maximum Error
WSP	− 90.08 dB	−33.93 dB	17.69 dB
GSP	−306.51 dB	− 99.12 dB	26.88 dB
BSP	−170.33 dB	− 67.17 dB	15.40 dB
USP	− 90.08 dB	−33.93 dB	17.69 dB

Maximum errors of −337.15dB and −20.17dB compared to other statistical distribution results. The comparison in this example of a small conductor shows that the proposed GSP method gives accurate moment matching compared to other statistical distributions.

The next example is a spiral inductor of order $n = 191$. The original system frequency response of the spiral inductor is plotted in FIGURE 4. The comparison of the ROM using the proposed GSP method with different statistical distributions is plotted in FIGURE 5. The absolute error comparison of the reduced model (order $p = 40$) for all distributions is plotted in FIGURE 6. The result shows a close match of the ROM using the GSP with the original system response and is further highlighted in TABLE 2. The GSP method shows a Minimum Mean error of −99.12dB as well as reduced Minimum and Maximum errors of −306.51 dB and 26.88 dB respectively. The results in TABLE 2 also show the lowest Mean, Minimum and Maximum error of −99.12dB, −306.51dB, and 26.88dB respectively by ROM generated by the proposed GSP method.

The last higher-order interconnect example is an RLC network of order 1202. The original system frequency response is plotted in FIGURE 7. Note that large variations are seen at the higher frequency response (frequency > 1Ghz) of the original system, which is natural to the extracted response of any on-chip interconnect model. The comparison of ROM by all distributions is shown in FIGURE 8. The ROM using

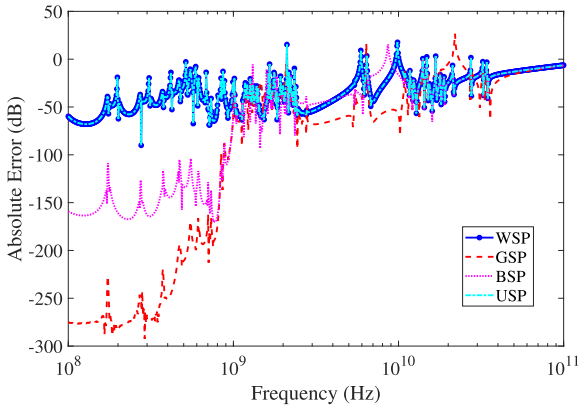

FIGURE 6. The absolute error of the reduced orders compared to the original system for the spiral inductor example using various statistical methods for the selection of spectral zeros. The calculated Mean absolute error is -33.93 dB, -99.12 dB, -67.17 dB, and -33.93 dB for WSP, GSP, BSP, and USP methods respectively.

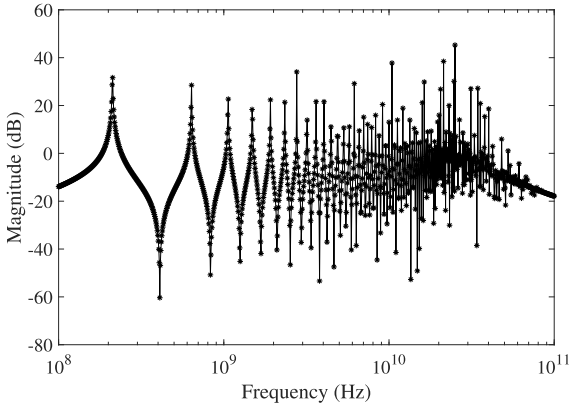

FIGURE 7. The response of an on-chip RLC network system with order $n = 1202$.

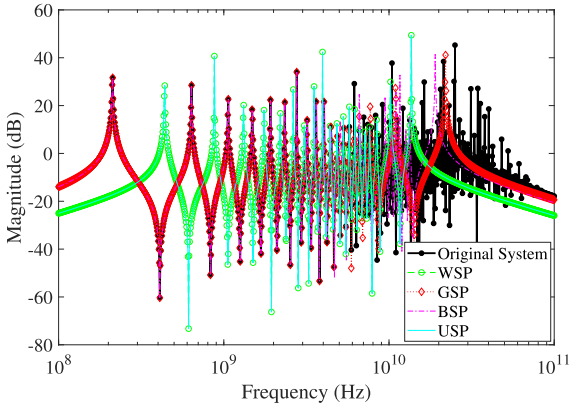

FIGURE 8. The response of an on-chip RLC network with the original order of $n = 1202$. The order of the reduced models using GSP, BSP, WSP, and USP is $k = 40$. The ROM generated by the GSP method shows a close match in comparison to other distributions.

selected SZs generated by the proposed GSP method accurately captures the behavior rather than binomial, weibull, and uniform distributions. The RLC absolute error is plotted in FIGURE 9. The error comparison is shown in TABLE 3, which further emphasizes the efficiency and accuracy of our suggested GSP method by displaying a minimum mean error of $-117.05\ dB$ compared to other distribution methods.

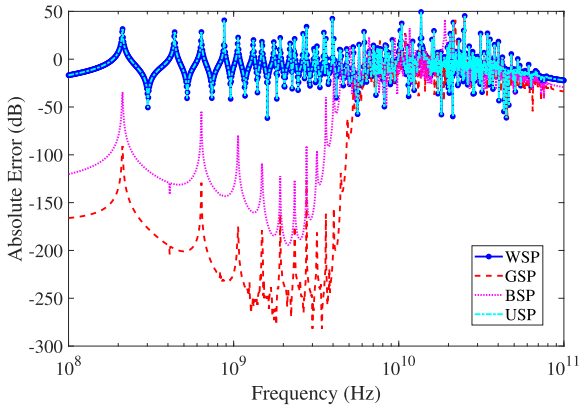

FIGURE 9. The absolute error of the reduced orders compared to the original system for the RLC network example using various statistical methods for the selection of spectral zeros. The calculated Mean absolute error is -8.27 dB, -117.05 dB, -73.86 dB, and -8.27 dB for WSP, GSP, BSP, and USP methods respectively.

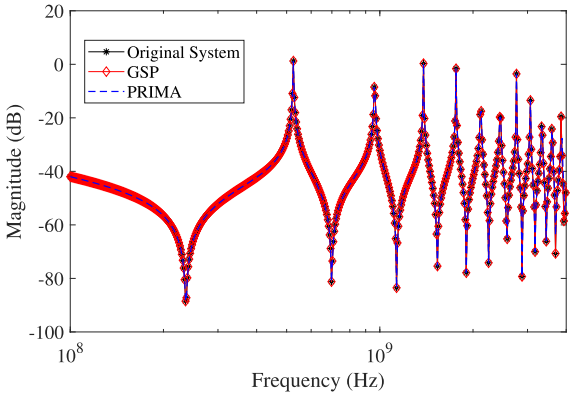

FIGURE 10. The response of a small conductor with original system order of $n = 79$. The ROM using GSP and PRIMA methods are of order $k = 40$.

TABLE 3. Error Comparison of RLC Network.

Distributions	Minimum Error	Mean Error	Maximum Error
WSP	− 61.60 dB	− 8.27 dB	49.41 dB
GSP	−284.90 dB	− 117.05 dB	45.21 dB
BSP	−194.16 dB	− 73.86 dB	45.24 dB
USP	− 61.60 dB	−8.27 dB	49.41 dB

In order to compare the results with previous techniques, a comparison of the projected ROM using the GSP method of order $k = 40$ and PRIMA [25] for the small conductor example is plotted in FIGURE 10. Note that the original order of the example is $n = 79$ and the result for reduced order shows a better response for both the PRIMA and GSP methods. However, a close look at the absolute error response in FIGURE 11 shows a better response from the GSP method in comparison to PRIMA.

In model order reduction, computational complexity plays an important role. Without loss of generality, we only compare the time taken in reducing (using the GSP algorithm) and simulating the ROM with the simulation time of the original system. The comparison for the three examples is given in Table 4. The comparison shows a significant improvement in saving computational time by applying the GSP algorithm and reducing the original model.

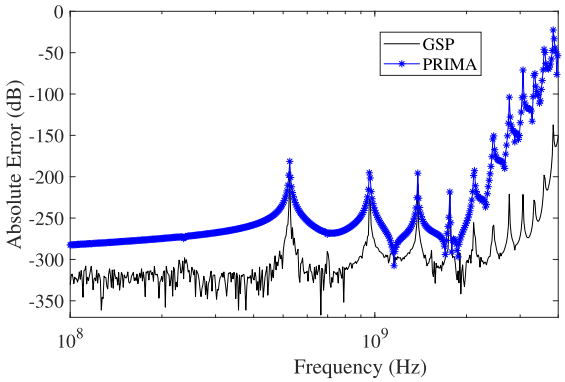

FIGURE 11. The absolute error of the reduced orders compared to the original system for the RLC network example using various statistical methods for the selection of spectral zeros. The calculated Mean absolute error is -8.27 dB, -117.05 dB, -73.86 dB, and -8.27 dB for WSP, GSP, BSP, and USP methods respectively.

TABLE 4. Comparison of Simulation Time.

Example	Original Order	Simulation time Original Order	Reduce Order using GSP	Simulation time (GSP Algorithm+ Reduce Order)
RLC-network	1202	328 seconds	40	161.66 + 0.22 seconds
Spiral Inductor	191	3.02 seconds	40	0.25 + 0.21 seconds
Small Conductor	79	0.69 seconds	40	0.038 + 0.25 seconds

V. CONCLUSION

MOR of an on-chip interconnect is an essential tool in determining the performance of very high-speed VLSI design systems. In this work, we developed a new gaussianly distributed spectral zero projection method of MOR. The results show that our method is both efficient and accurate and produces stable ROM. In addition, the ROM preserves the passivity and stability and can be used successfully to approximate large-scale interconnect systems to mitigate the design complexity challenges for the development and fabrication of modern integrated circuits.

APPENDIX. RATIONAL FUNCTION AND STATE-SPACE SYSTEM REPRESENTATION

In science and engineering, quite often the original system is given either in state space or a rational function representation. Consider the following system representation

$$\begin{aligned} C_{cell}\dot{x} &= G_{cell}x(t) + B_{cell}u(t), \\ y(t) &= L_{cell}x(t) + D_{cell}u(t). \end{aligned} \tag{15}$$

Applying Laplace Transform

$$\begin{aligned} sC_{cell}X(s) &= G_{cell}X(s) + B_{cell}U(s), \\ Y(s) &= L_{cell}X(s) + D_{cell}U(s). \end{aligned} \tag{16}$$

Let us solve the rational function $P(s) = \dfrac{Y(s)}{U(s)}$, and first derive the value of X(s) from the input equation.

$$X(s) = (sC_{cell} - G_{cell})^{-1}B_{cell}U(s).$$

Using $X(s)$, $Y(s)$ can be expressed as

$$Y(s) = L_{cell}(sC_{cell} - G_{cell})^{-1}B_{cell}U(s) + D_{cell}U(s),$$
$$= \left(L_{cell}(sC_{cell} - G_{cell})^{-1}B_{cell} + D_{cell}\right)U(s).$$

Now, we can solve this for the rational function $P(s)$ and can write

$$P(s) = \frac{Y(s)}{U(s)}$$
$$= L_{cell}(sC_{cell} - G_{cell})^{-1}B_{cell} + D_{cell}. \quad (17)$$

Similarly, a rational function 17 can also be converted into state space form 15. Assuming zero initial conditions, the process entails converting the rational function to a differential equation and performing an inverse Laplace transform. The differential equation is then expressed in state space form.

REFERENCES

[1] N. A. Sherwani, *Algorithms for VLSI Physical Design Automation*. Springer, 2012.
[2] S. Kundu and S. Chattopadhyay, *Network-on-Chip: The Next Generation of System-on-Chip Integration*. New York, NY, USA: Taylor & Francis, 2014.
[3] B. Gugulothu, B. R. Naik, and S. Boodidha, "Modeling of capacitive coupled interconnects for crosstalk analysis in high speed VLSI circuits," in *Proc. Int. Conf. Commun. Signal Process. (ICCSP)*, Apr. 2019, pp. 7–11.
[4] G. Ciuprina and D. Ioan, *Scientific Computing in Electrical Engineering*, vol. 11. Springer, 2007.
[5] M. Alam, A. Nieuwoudt, and Y. Massoud, "Frequency selective model order reduction via spectral zero projection," in *Proc. Asia South Pacific Des. Autom. Conf.*, Jan. 2007, pp. 379–383.
[6] F. Y. M. Wan, *Mathematical Models and Their Analysis*. Philadelphia, PA, USA: SIAM, 2018.
[7] R. Malik, M. Alam, S. Muhammad, R. Hussain, A. Ali, N. Akram, F. Z. Duraihem, and A. U. Haq, "Statistically inspired multi-shift Arnoldi projection for on-chip interconnects," *Math. Comput. Simul.*, vol. 190, pp. 418–428, Dec. 2021.
[8] M. Bakhouya, S. Suboh, J. Gaber, T. El-Ghazawi, and S. Niar, "Performance evaluation and design tradeoffs of on-chip interconnect architectures," *Simul. Model. Pract. Theory*, vol. 19, no. 6, pp. 1496–1505, Jun. 2011.
[9] R. Malik, M. Alam, S. Muhammad, F. Z. Duraihem, and Y. Massoud, "Second-order Arnoldi reduction using weighted Gaussian kernel," *IEEE Access*, vol. 10, pp. 41362–41370, 2022.
[10] U. Baur, P. Benner, and L. Feng, "Model order reduction for linear and nonlinear systems: A system-theoretic perspective," *Arch. Comput. Methods Eng.*, vol. 21, no. 4, pp. 331–358, Dec. 2014.
[11] A. C. Antoulas, *Approximation of Large-Scale Dynamical Systems*. Philadelphia, PA, USA: SIAM, 2005.
[12] W. H. A. Schilders, H. A. Vorst, and J. Rommes, *Model Order Reduction: Theory, Research Aspects and Applications*. Springer, 2008, vol. 13.
[13] P. Feldmann, "Model order reduction techniques for linear systems with large numbers of terminals," in *Proc. Design, Autom. Test Eur. Conf., Exhib.*, vol. 2, Feb. 2004, pp. 944–947.
[14] R. Malik, M. Alam, and S. Muhammad, "Approximation of large-scale system using equivalent-norm frequency selected projection," in *Proc. 19th Int. Bhurban Conf. Appl. Sci. Technol. (IBCAST)*, Aug. 2022, pp. 523–527.
[15] S. Gugercin, *Projection Methods for Model Reduction of Large-Scale Dynamical Systems*. Houston, TX, USA: Rice Univ., 2003.
[16] X.-L. Wang and Y.-L. Jiang, "Two-sided projection methods for model reduction of MIMO bilinear systems," *Math. Comput. Model. Dyn. Syst.*, vol. 19, no. 6, pp. 575–592, Dec. 2013.
[17] M. Alam, *Compact Models for Nanophotonic Structures and On-Chip Interconnects*. Houston, TX, USA: Rice Univ., 2007.
[18] S. K. Chaudhary and A. Kumar, "Hankel norm approximation of a stable non-minimal system," in *Proc. 1st Int. Conf. Electron., Mater. Eng. Nano-Technol. (IEMENTech)*, Apr. 2017, pp. 1–4.
[19] A. Nieuwoudt, M. Alam, and Y. Massoud, "Reduced-order wide-band interconnect model realization using filter-based spline interpolation," in *Proc. Asia South Pacific Des. Autom. Conf.*, Jan. 2007, pp. 373–378.
[20] A. C. Antoulas, R. Ionutiu, N. Martins, E. J. W. T. Maten, K. Mohaghegh, R. Pulch, J. Rommes, M. Saadvandi, and M. Striebel, "Model order reduction: Methods, concepts and properties," in *Coupled Multiscale Simulation and Optimization in Nanoelectronics*. Springer, 2015, pp. 159–265.
[21] M. Alam, A. Nieuwoudt, and Y. Massoud, "Wavelet-based passivity preserving model order reduction for wideband interconnect characterization," in *Proc. 8th Int. Symp. Quality Electron. Design (ISQED)*, Mar. 2007, pp. 432–437.
[22] U. Zulfiqar, W. Tariq, L. Li, and M. Liaquat, "A passivity-preserving frequency-weighted model order reduction technique," *IEEE Trans. Circuits Syst. II, Exp. Briefs*, vol. 64, no. 11, pp. 1327–1331, Nov. 2017.
[23] Y. Massoud, M. Alam, and A. Nieuwoudt, "On the selection of spectral zeros for generating passive reduced order models," in *Proc. 6th Int. Workshop Syst. Chip Real Time Appl.*, Dec. 2006, pp. 160–164.
[24] M. Alam, A. Nieuwoudt, and Y. Massoud, "Dynamic multi-point rational interpolation for frequency-selective model order reduction," in *Proc. IEEE Dallas/CAS Workshop Design, Appl., Integr. Softw.*, Oct. 2006, pp. 95–98.
[25] A. Odabasioglu, M. Celik, and L. T. Pileggi, "PRIMA: Passive reduced-order interconnect macromodeling algorithm," *IEEE Trans. Comput. Aided Design Integr. Circuits Syst.*, vol. 17, no. 8, pp. 645–654, Aug. 1998.
[26] R. W. Freund, "Krylov-subspace methods for reduced-order modeling in circuit simulation," *J. Comput. Appl. Math.*, vol. 123, nos. 1–2, pp. 395–421, Nov. 2000.
[27] M. Alam, A. Nieuwoudt, and Y. Massoud, "Model order reduction using spline-based dynamic multi-point rational interpolation for passive circuits," *Anal. Integr. Circuits Signal Process.*, vol. 50, no. 3, pp. 273–277, Feb. 2007.
[28] R. W. Freund, "SPRIM: Structure-preserving reduced-order interconnect macromodeling," in *Proc. IEEE/ACM Int. Conf. Comput. Aided Design (ICCAD)*, Nov. 2004, pp. 80–87.
[29] M. Alam, A. Nieuwoudt, and Y. Massoud, "Efficient multi-shifted Arnoldi projection using wavelet transform," *J. Circuits, Syst. Comput.*, vol. 16, no. 5, pp. 699–709, Oct. 2007.
[30] S. Tan and L. He, *Advanced Model Order Reduction Techniques in VLSI Design*. Cambridge, U.K.: Cambridge Univ. Press, 2007.
[31] M. Alam, A. Nieuwoudt, and Y. Massoud, "Provably passive second order model order reduction for package parasitics using spectral zeros," in *Proc. IEEE Northeast Workshop Circuits Syst.*, Aug. 2007, pp. 791–794.
[32] L. M. Silveira, M. Kamon, I. Elfadel, and J. White, "A coordinate-transformed Arnoldi algorithm for generating guaranteed stable reduced-order models of RLC circuits," *Comput. Methods Appl. Mech. Eng.*, vol. 169, nos. 3–4, pp. 377–389, Feb. 1999.
[33] H. Zheng and L. T. Pileggi, "Robust and passive model order reduction for circuits containing susceptance elements," in *Proc. IEEE/ACM Int. Conf. Comput. Aided Design (ICCAD)*, Nov. 2002, pp. 761–766.
[34] Q. Su, V. Balakrishnan, and C.-K. Koh, "Efficient approximate balanced truncation of general large-scale RLC systems via Krylov methods," *Methods*, vol. 4, p. 5, 2002.
[35] Y. I. Ismail, "Evaluating noise pulses in RC networks due to capacitive coupling," in *Proc. IEEE Int. Symp. Circuits Syst. (ISCAS)*, May 2002, p. 5.
[36] J. R. Phillips and L. M. Silveira, "Poor man's TBR: A simple model reduction scheme," *IEEE Trans. Comput. Aided Des. Integr. Circuits Syst.*, vol. 24, no. 1, pp. 43–55, Jan. 2005.
[37] L. M. Silveira and J. R. Phillips, "Exploiting input information in a model reduction algorithm for massively coupled parasitic networks," in *Proc. 41st Annu. Design Autom. Conf.*, Jul. 2004, pp. 385–388.
[38] J. R. Phillips, L. Daniel, and L. M. Silveira, "Guaranteed passive balancing transformations for model order reduction," *IEEE Trans. Comput. Aided Design Integr. Circuits Syst.*, vol. 22, no. 8, pp. 1027–1041, Aug. 2003.
[39] C. R. Vogel and J. G. Wade, "Iterative SVD-based methods for ill-posed problems," *SIAM J. Sci. Comput.*, vol. 15, no. 3, pp. 736–754, May 1994.
[40] A. C. Antoulas, "A new result on passivity preserving model reduction," *Syst., Control Lett.*, vol. 54, no. 4, pp. 361–374, Apr. 2005.
[41] D. C. Sorensen, "Passivity preserving model reduction via interpolation of spectral zeros," *Syst., Control Lett.*, vol. 54, no. 4, pp. 347–360, Apr. 2005.

[42] R. Ionutiu, J. Rommes, and A. C. Antoulas, "Passivity-preserving model reduction using dominant spectral-zero interpolation," *IEEE Trans. Comput. Aided Design Integr. Circuits Syst.*, vol. 27, no. 12, pp. 2250–2263, Dec. 2008.
[43] N. Akram, M. Alam, R. Hussain, A. Ali, S. Muhammad, R. Malik, and A. U. Haq, "Passivity preserving model order reduction using the reduce norm method," *Electronics*, vol. 9, no. 6, p. 964, Jun. 2020.
[44] X. Wang, M. Yu, and C. Wang, "Structure-preserving-based model-order reduction of parameterized interconnect systems," *Circuits, Syst., Signal Process.*, vol. 37, no. 1, pp. 19–48, Jan. 2018.
[45] L. Benini and G. de Micheli, *Dynamic Power Management: Design Techniques and CAD Tools*. Springer, 1998.
[46] K. Nabors and J. White, "FastCap: A multipole accelerated 3-D capacitance extraction program," *IEEE Trans. Comput. Aided Design Integr. Circuits Syst.*, vol. 10, no. 11, pp. 1447–1459, Nov. 1991.
[47] M. Kamon, M. J. Tsuk, and J. K. White, "FASTHENRY: A multipole-accelerated 3-D inductance extraction program," *IEEE Trans. Microw. Theory Techn.*, vol. 42, no. 9, pp. 1750–1758, Sep. 1994.
[48] *Fast Field Solvers, FastCap, FastHenry, FasterCap, FastImp, and FastFieldsolvers*. [Online]. Available: https://www.fastfieldsolvers.com/
[49] R. Ionutiu, S. Lefteriu, and A. C. Antoulas, "Comparison of model reduction methods with applications to circuit simulation," in *Scientific Computing in Electrical Engineering*. Springer, 2007, pp. 3–24.
[50] R. Ionutiu, "Model reduction for descriptor systems with applications to circuit simulation," William Marsh Rice Univ., Houston, TX, USA, Tech. Rep. TREE07-07, 2007.
[51] V. Mehrmann and T. Stykel, "Balanced truncation model reduction for large-scale systems in descriptor form," in *Dimension Reduction of Large-Scale Systems*. Springer, 2005, pp. 83–115.

NAMRA AKRAM received the B.Sc. degree in mathematics and physics from the University of Azad Jammu and Kashmir, Muzaffarabad, Pakistan, and the M.Sc. (Hons.) and M.Phil. degrees in mathematics from the Mirpur University of Science and Technology, Mirpur, Pakistan, in 2014 and 2016, respectively, where she is currently pursuing the Ph.D. degree in mathematics. Her research interest includes passivity preserving model order reduction techniques for large-scale dynamical linear systems.

MEHBOOB ALAM (Member, IEEE) received the B.S. degree (Hons.) from the University of Engineering and Technology, Lahore, Pakistan, the M.Sc. degree in electrical and computer engineering from the University of Calgary, Calgary, AB, Canada, in 2003, and the Ph.D. degree in electrical and computer engineering from Rice University, Houston, TX, USA, in 2007. He was an NSERC Postdoctoral Fellow with the Department of Electrical and Computer Engineering, University of Toronto, Canada. He is currently an Associate Professor with the Department of Electrical Engineering, University of Poonch Rawalakot, Pakistan. He was a recipient of the Informatics Circle of Research Excellence (iCORE) Canada Postgraduate Scholarship (2002–2003). He received the Canadian Strategic Microelectronics Council of ITAC Industrial Collaboration Award (SMC Award), in 2003.

RASHIDA HUSSAIN received the Ph.D. degree from the University of Graz, Austria. She is currently a Professor and the Chairperson with the Department of Mathematics, Mirpur University of Science and Technology, Mirpur, Pakistan. Her research interests include mathematical modeling, differential equations, inequalities, and fluid mechanics.

YEHIA MASSOUD (Fellow, IEEE) received the Ph.D. degree in electrical engineering and computer science from the Massachusetts Institute of Technology (MIT), Cambridge, MA, USA. He has held several positions at leading institutions of higher education and the industry, including Rice University, the Stevens Institute of Technology, USA, Worcester Polytechnic Institute (WPI), UAB, the SLAC National Accelerator Laboratory, and Synopsys Inc. In 2003, he joined Rice University, as an Assistant Professor, where he became one of the fastest Rice Faculty to be granted tenure in electrical and computer engineering and computer science, in 2007. From January 2018 to July 2021, he was the Dean of the School of Systems and Enterprises (SSE), Stevens Institute of Technology. Before the Stevens Institute of Technology, he was the Head of the Department of Electrical and Computer Engineering (ECE), WPI, from 2012 to 2017. He is currently the Director of Innovative Technologies Laboratories (ITL), King Abdullah University of Science and Technology (KAUST). He has been a PI or a Co-PI on more than U.S. $30 million of funded research from the NSF, DOD, SRC, and the industry. His research group was responsible for developing the world's first realization of compressive sensing systems for signals, which provided an unprecedented one-order of magnitude savings in power consumption and significant reductions in size and cost and has enabled the implementation of self-powered sensors for smart cities and ultra-low-power biomedical implantable devices. He has published more than 400 papers in leading peer-reviewed journals and conference publications. His research interests include the design of state-of-the-art innovative technological solutions that span a broad range of technical areas, including smart cities, autonomy, smart health, smart mobility, embedded systems, nanophotonics, and spintronics. He was selected as one of the ten MIT Alumni Featured by the Electrical Engineering and Computer Science Department, MIT, in 2012. He was a recipient of the Rising Star of Texas Medal, the National Science Foundation CAREER Award, the DAC Fellowship, the Synopsys Special Recognition Engineering Award, and several best paper awards. He has served on the IEEE CAS Award Nomination Committee, the IEEE Mac Valkenburg Award Committee, the IEEE CAS Fellow Committee, the IEEE Rebooting Computing Steering Committee, and the IEEE Nanotechnology Council. He also served as the 2016 IEEE MWSCAS Technical Program Co-Chair, the 2009 General Program Co-Chair, and the 2007 Technical Program Co-Chair for the ACM Great Lakes Symposium on VLSI. He has served as the Editor for the *Mixed-Signal Letters—The Americas*, an Associate Editor for the IEEE TRANSACTIONS ON VERY LARGE SCALE INTEGRATION (VLSI) SYSTEMS and the IEEE TRANSACTIONS ON CIRCUITS AND SYSTEMS—I: REGULAR PAPERS, and the Guest Editor for a Special Issue of the IEEE TRANSACTIONS ON CIRCUITS AND SYSTEMS—I: REGULAR PAPERS. He was also named a Distinguished Lecturer by the IEEE Circuits and Systems Society.